Supplementary Information

Pt-TiO_2 catalysts for glycerol photoreforming: comparison of anatase, brookite and rutile polymorphs

Claudio Maria Pecoraro,[a] Lorenzo Mino,[*b] Elizaveta Kozyr,[b] Leonardo Palmisano,[a] Francesco di Franco,[a] Vittorio Loddo,[a] Monica Santamaria,[a] Marianna Bellardita[*a]

[a]Engineering Department, University of Palermo, Viale delle Scienze Ed. 6, Palermo, 90128, Italy. E

[b]Department of Chemistry and Interdepartmental Centre NIS, University of Torino, Via Giuria 7, 10125 Torino, Italy.

*Corresponding authors e-mail: lorenzo.mino@unito.it; marianna.bellardita@unipa.it

Samples preparation

Home prepared Pt-TiO_2 samples displaying different phase where prepared and compared for the photoreformig of glucose. Commercial TiO_2 P25 was used as reference.

Titanium tetrachloride (Fluka 98%) and titanium(IV) oxysulfate (Sigma-Aldrich ≥29% Ti,(as TiO_2) were used as received as TiO_2 precursors whilst $PtCl_4$ (Sigma-Aldrich 96%) as Pt source.

TiO_2 anatase was prepared by adding 40 g of $TiOSO_4$ to 180 mL of distilled water and stirring the resulting mixture for ca. 2 h at room temperature until a clear solution was formed. The latter was transferred in a closed bottle and treated for 48 h at 373 K in an oven. The resulting precipitate was washed twice with water to eliminate the sulphate ions, dried at 323 K and calcined for 3 h at 873 K.

TiO_2 brookite was obtained by introducing 210 mL of demineralized water, 80 mL of HCl and 5 mL of $TiCl_4$ into a Pyrex bottle that was closed and aged in an oven for 48 h at 373 K. A precipitate containing a mixture of brookite and rutile was obtained. Pure brookite was separated from rutile by peptization with water and dried under vacuum at 323 K.

TiO_2 rutile was synthesized by adding, under stirring at room temperature, 20 mL of $TiCl_4$ to 100 ml of distilled water. The obtained solution was heated in an oven at 373 K for 48 h in a closed bottle. The solid was recovered by dryng in a rotary evaporator at 323 K. Pt (0.5% wt) was loaded on TiO_2 by a photodeposition method.

Samples characterization

X-Ray diffraction (XRD) patterns of the various samples were obtained by a PANalytical Empyrean diffractometer operating a current of 30 mA and at a voltage of 40 kV by using the CuKa radiation. The crystalline sizes of the powders were calculated by using the Scherrer equation.

Raman spectra were acquired by means of BWTek-i-micro Raman Plus System using a 532 nm laser. The spectra were collected in the 125-1000 cm^{-1} Raman shift range and every measure was the average of two repetitions.

The specific surface areas (SSA) were calculated by a Micromeritics Flow Sorb 2300 apparatus by using the single-point BET method.

The Diffuse Reflectance Spectra (DRS) were acquired by a Shimadzu UV-2401 PC spectrophotometer in the 200-800 nm wavelength range. $BaSO_4$ was used as the reference sample. Band gap values were calculated by plotting the modified Kubelka-Munk function, $[F(R'_\infty)hv]^{1/2}$, versus the energy of the exciting light.

Scanning electron microscopy (SEM) images were acquired by a FEI Quanta 200 ESEM microscope operating at 30 kV. An electron microprobe used in an energy dispersive mode (EDX) was employed to investigate the elementary composition of the samples.

Fourier-transform infrared spectroscopy measurements (FT-IR) were performed using a Bruker INVENIO-R spectrometer (resolution: 2 cm^{-1}; detector: DTGS), averaging 128 scans. For the *in situ* experiments, an aliquot of each type of TiO_2 nanoparticles was pressed in self-supporting pellets ("optical density" of ca. 10 $mg \cdot cm^{-2}$) and placed in quartz cells equipped with KBr windows designed to carry out spectroscopic measurements in controlled atmosphere. Before CO adsorption, the TiO_2 samples were activated with the following procedure: (i) outgassing at 673 K for 30 min; (ii) contacting twice with 10 mbar of O_2 for 10 min at the same temperature; (iii) cooling to 423 K in O_2, then outgassing for 10 min; (iv) contacting with 15 mbar of H_2 at 423 K for 10 min; and (v) cooling from 423 K to room temperature under outgassing.

Photocatalytic activity evaluation

Glycerol, glyceraldehyde and 1,3-dihydroxyacetone were purchased by Sigma Aldrich and used as received. The photocatalytic runs were carried out in a cylindrical Pyrex reactor containing 150 mL of an aqueous glycerol (2mM) dispersion in anaerobic conditions. Both a 125 W medium pressure Hg lamp (main emission peak at 365 nm) and a 150 W halogen lamp (simulating the solar spectrum) were used as irradiation sources. Helium was bubbled in the suspension for 0.5 h under dark, then

the reactor was sealed, and the lamp switched on. Water was circulated in the reactor jacket to keep the temperature of the suspension at about 303 K. To analyse the reaction mixture composition, aliquots were withdrawn at fixed times, filtered through 0.2 µm PTFE membranes and analysed by a Thermo Scientific Dionex UltiMate 3000 HPLC equipped with a Diode Array detector. A REZEK ROA Organic acid H^+ column, crossed by an aqueous $2.5 \cdot 10^{-3}$ M H_2SO_4 solution at a flow rate of 0.6 mL·min^{-1}, was used to separate the different compounds. An HP 6890 Series GC System equipped with a Supelco GC 60/80 Carboxen^{TM}-1000 packed column and a thermal conductivity detector was used to analyse CO_2 and H_2 accumulated in the reactor headspace.

The following equations were used for the determination of X (Glycerol conversion), S (selectivity):

$$X = \frac{[Glycerol]i - [Glycerol]t}{[Glycerol]i} * 100$$

$$S = \frac{[P]t}{[Glycerol]i - [Glycerol]t} * 100$$

where: [Glycerol]i and [Glycerol]t indicate the initial molar concentration and molar concentration at time t of the glycerol, respectively. [P]t is the molar concentration of the obtained product (DHA or GA) at time t.

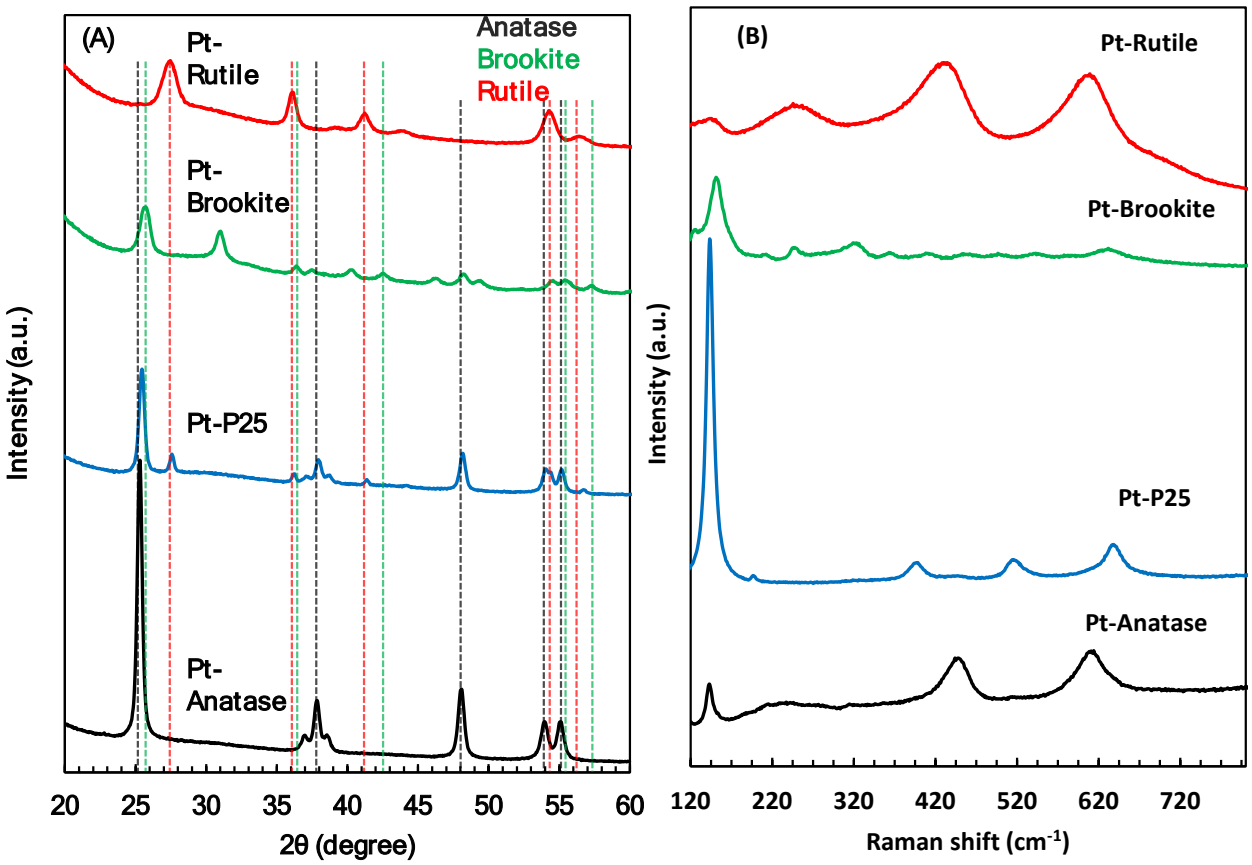

Figure S1. (A) XRD patterns and (B) Raman spectra of the different samples. A) Anatasio: JCPDS Card No 21-1272, 2θ: 25.2° 37.3° 47.6° 53.5° 55.1° 62.2°[1]. Rutilo: JCPDS Card no. 21-1276, 2θ: 27.0° 35.6° 40.8° 54.0° 53.9° 56.1°[1] and 61.0°. Brookite: JCPDS card no. 29-1360, 2θ: 25.3° 25.7° 36.2° 42.3° 55.2° 57.2°[2]

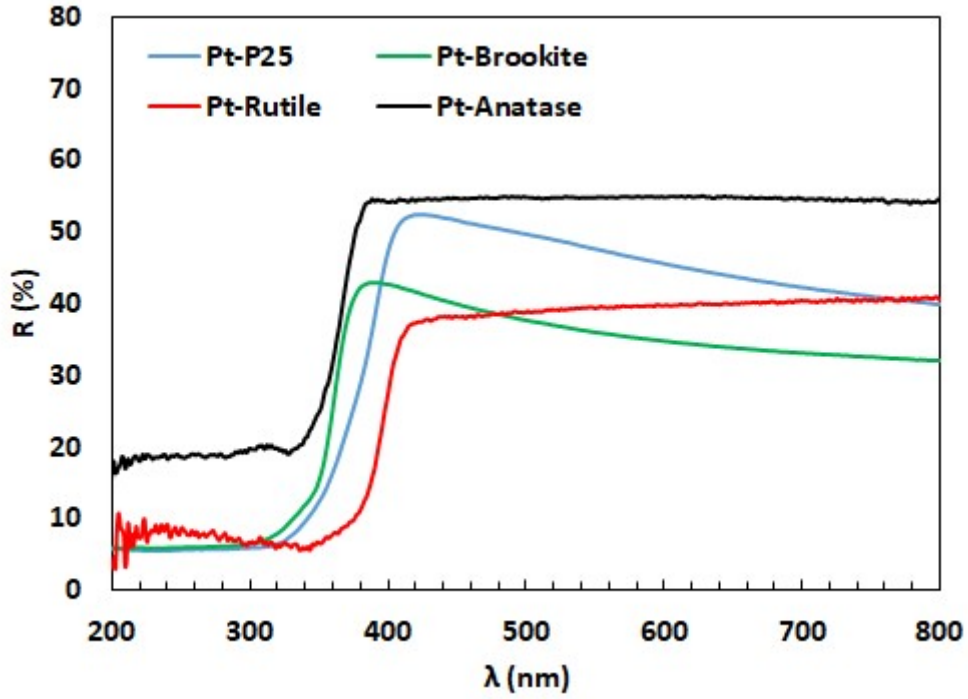

Figure S2. Diffuse reflectance UV-Vis spectra of the different samples.

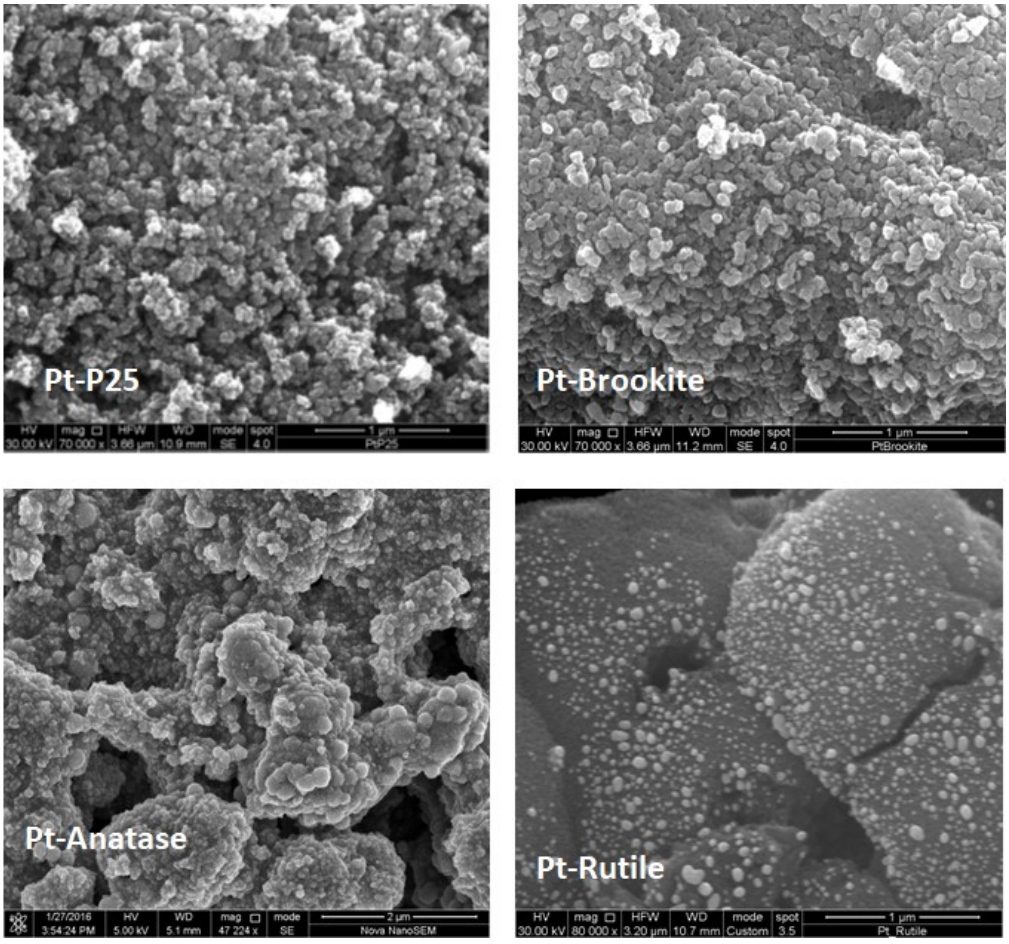

Figure S3. SEM images of the different samples.

The results for Pt-Brookite reported in Table S1 show that by increasing glycerol concentration the conversion decreased and, consequently, the selectivity increased. Moreover, the amount of glycerol converted increased together with the amount of H_2 and CO_2. The higher H_2 amount can be due both the higher amount of reacted glycerol and to the to the greater number of H_2O molecules broken due to the greater number of available electrons. In fact, the increased quantity of holes used to convert more glycerol corresponds to a greater number of electrons available for the reduction of H^+ ions.

Table S1. Photocatalytic results for Pt-Brookite obtained after 4 h of UV light irradiation at two different glycerol concentrations. X = glycerol conversion, S = selectivity. DHA = 1,3-dihydroxyacetone, GA = glyceraldehyde.

Glycerol (mM)	X (%)	S_{DHA} (%)	S_{GA} (%)	CO_2 (mM)	H_2 (mM)	H_2/CO_2	Glycerol converted (mmol)
2	26	6.8	8.1	0.23	9.3	40.4	0.095
5	19.3	8.48	14.5	0.39	12.3	31.5	0.14

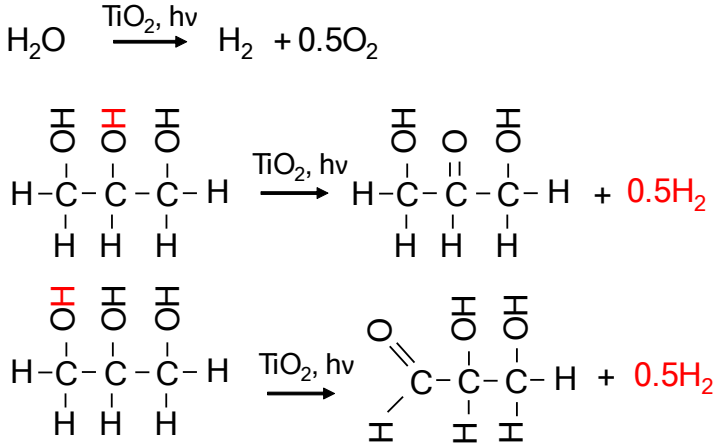

Scheme S1. Main products from photocatalytic glycerol reforming.

A run in the presence of tert-butanol 1 mM (as ·OH scavenger in accordance with literature [3]) by using Pt-Brookite was carried out (Figure S4). No substantial variations in the glycerol degradation during irradiation can be noticed. This finding indicates that, in this case, hydroxyl radicals (·OH) are not the main species involved in the glycerol degradation.

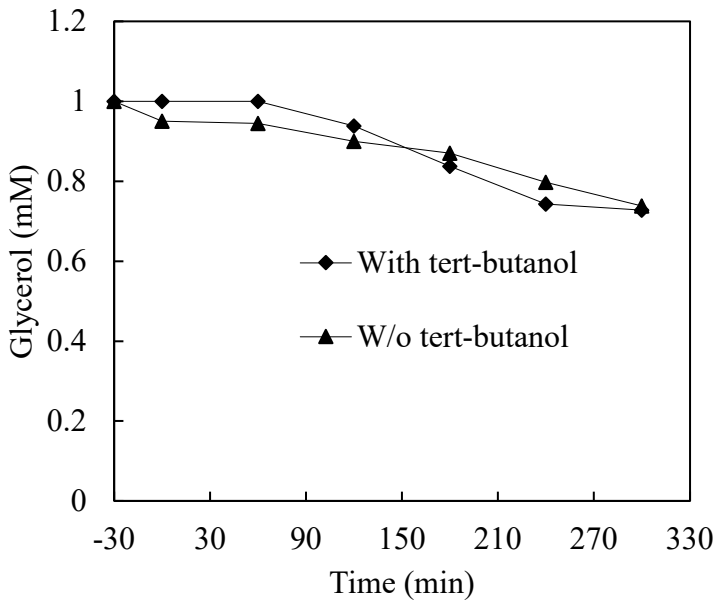

Figure S4. Photocatalytic degradation of glycerol with Pt-Brookite in the presence of tert-butanol as ·OH scavenger.

In Table S2 the data obtained during the photocatalytic degradation of glycerol with different TiO_2-based samples are reported. In same investigation both the products deriving from glycerol partial oxidation and H_2 are evaluated, in some only one of them. Pure Brookite (modified with Pt), used for the first time for glycerol photoreforming, showed an activity comparable (sometimes higher) to that reported in the literature for the other TiO_2 polymorphs. The results are encouraging although the aim of this communication was not the optimization of H_2 production, but to elucidate the relationship between some properties of the catalysts and their photoactivity.

Table S2. Performance comparison of different TiO_2-based samples.

Catalyst	**Conditions**	**X (%)**	**S (%)**	**H_2**	**CO_2**	**Ref.**
Pt-Brookite	2 mM glycerol concentration 4h UV irradiation (125 W) 25 °C	26	DHA 6.8 GA 8.1	9300 µmol L^{-1}	230 µmol L^{-1}	This work
	4h simulated solar light irradiation (150 W) 25 °C	21	DHA 9.1 GA 10.0	5400 µmol L^{-1}	180 µmol L^{-1}	
Pt-TiO_2-Nb_2O_5	5 wt% glycerol concentration 4h UV irradiation			4710 µmol L^{-1}	241 µmol L^{-1}	4
NiO/TiO_2	2.28 M glycerol concentration 8h 500 W high-pressure Hg lamp 50 °C			1230 µmol g^{-1} h^{-1}		5
Pt-TiO_2	1 M glycerol concentration		GA 34	10000		6

	simulated solar light irradiation (300 W Xe-lamp) 30 °C		GlA 66	µmol g^{-1} h^{-}		
Cu_2O/TiO_2	2 mM glycerol concentration 5h UV irradiation (125 W) 25 °C	33	DHA 10.0 GA 5.4	1010 µmol L^{-1}	170 µmol L^{-1}	7
Pt-Rutile	20 mM glycerol concentration 8h Xe-lamp (300 W) 80 °C	11.6	HAA 93.2 GA 2.6	2453 µmol	1720 µmol	8
TiO_2	10 mM 6.5 h six 15W UV Neon 25 °C	35	DHA 6.5 GA 10 FA 3.1			9
Pt-N-TiO_2	10% vol glycerol concentration 5h simulated solar light irradiation (250 W)			3017 µmol		10

DHA = dihydroxyacetone; GA = glyceraldehyde; GlA = glycolaldehyde, HAA = Hydroxyacetaldehyde; FA = formic acid

References

1 W. Li, R. Liang, A. Hu, Z. Huang and Y. N. Zhou, *RSC Adv.*, 2014, **4**, 36959–36966.

2 S. Phromma, T. Wutikhun, P. Kasamechonchung, T. Eksangsri and C. Sapcharoenkun, *Applied Sciences*, 2020, **10**, 993.

3 Y. Ye, Y. Feng, H. Bruning, D. Yntema and H. H. M. Rijnaarts, *Appl Catal B*, 2018, **220**, 171–181.

4 G. Iervolino, V. Vaiano, J. J. Murcia, A. E. Lara, J. S. Hernández, H. Rojas, J. A. Navío and M. C. Hidalgo, *Int J Hydrogen Energy*, 2021, **46**, 38678–38691.

5 S. ichiro Fujita, H. Kawamori, D. Honda, H. Yoshida and M. Arai, *Appl Catal B*, 2016, **181**, 818–824.

6 V. Maslova, A. Fasolini, M. Offidani, S. Albonetti and F. Basile, *Catal Today*, 2021, **380**, 147–155.

7 C. M. Pecoraro, M. Bellardita, V. Loddo, F. Di Franco, L. Palmisano and M. Santamaria, *Journal of Industrial and Engineering Chemistry*, 2023, **118**, 247–258.

8 R. Chong, J. Li, X. Zhou, Y. Ma, J. Yang, L. Huang, H. Han, F. Zhang and C. Li, *Chemical Communications*, 2014, **50**, 165–167.

9 V. Augugliaro, H. A. H. El Nazer, V. Loddo, A. Mele, G. Palmisano, L. Palmisano and S. Yurdakal, *Catal Today*, 2010, **151**, 21–28.

10 Slamet, D. Tristantini, Valentina and M. Ibadurrohman, *Int J Energy Res*, 2013, **37**, 1372–1381.